Physical insights on graphene nanoribbon mobility through atomistic simulations

A. Betti, G. Fiori, G. Iannaccone, and *Y. Mao
Dipartimento di Ingegneria dell'Informazione
Università di Pisa, Via Caruso I-56122 Pisa, Italy
Tel. +39 050 2217639; Fax. +39 050 2217522, email: alessandro.betti@iet.unipi.it
*Dana Farber Cancer Institute Pathology, Jimmy Fund Bldg 61944 Binney St, Boston, MA 02115

***Abstract*— We present an investigation of the main mechanisms which limit mobility in GNR-FETs, by means of atomistic simulations based on the NEGF formalism. In particular, we focus on *i)* line edge roughness (LER), *ii)* single defects; *iii)* ionized impurities, *iv)* acoustic and optical phonons. Results show that the effect of ionized impurities is negligible, while phonons, LER and defects largely limits carrier mobility, especially for narrower GNRs.**

I. Introduction

Graphene has recently demonstrated really intriguing electrical properties such as high carrier mobility [1], [2] and large coherence lengths [3]. However mobility measurements reported in literature exhibit extreme variability (from 10^2 to 10^4 cm^2/Vs) posing several questions on the main mechanisms affecting carrier transport in graphene.

The scenario even worsens in GNRs [4], [5], where line edge roughness (LER) additionally plays an important role, due to the extreme challenges in patterning nanoribbons.

In this framework, numerical simulation can certainly help to understand the role of the different scattering mechanisms, clarifying some unsolved issues and in order to overcome the severe lack of experiments. Efforts based on an analytical method [6] and on Monte Carlo approach [7] have been directed towards the goal of achieving a physical insight in GNRs mobility. However, due to the reduced dimensions of the considered material, effects at the atomistic scale are relevant, so that accurate simulation approaches like semi-empirical tight-binding have to be exploited.

In this work we present atomistic simulations of GNR-FETs over a wide range of GNR widths (1 to 10 nm) including LER, defects, ionized impurities as well as acoustic and optical phonons. In particular, our approach is based on statistical simulations performed on large ensembles of actual distribution of non-idealities. To this purpose, we have extensively used our parallelized 3D device simulator NANOTCAD ViDES, based on the self-consistent solution of the 3D Poisson and Schrödinger equations within the NEGF framework, and on a p_z tight-binding Hamiltonian [8].

II. Methodology

Mobility is strictly defined in infinitely long structures. In practice, we have considered finite channel segments, enforcing at both ends null Neumann boundary conditions on the potential, and open boundary conditions for travelling electrons.

Mobility has been computed from statistical simulations of resistance on an ensemble of about 100 nanoribbon segments with different actual distributions of non-idealities as

$$\mu_n = \frac{L^2}{\langle (R_{ch,i} - R_B)\, Q_i \rangle}\,, \tag{1}$$

where L is the segment length, Q_i and $R_{ch,i}$ are the total charge and the resistance of the i-th simulated GNR segment, respectively, R_B is the resistance of a ballistic segment in the same bias conditions and $\langle\,\rangle$ denotes the statistical average on the ensemble.

Defects have been modeled computing the on-site energy and the hopping parameter of the Hamiltonian from DFT calculations [9]. In particular, for a fixed defect concentration n_d, a defect distribution have been obtained by extracting in correspondence of each carbon atom a random number r uniformly distributed between 0 and 1 and by imposing a single vacancy on the carbon site if $r < n_d$. For what concerns LER, edge-disordered ribbons have been obtained by randomly removing atoms on the two outermost dimer lines. In particular, each atom has a probability H of being removed, where H is the fraction of edge disorder, defined as the ratio between the number of edge defects and the total number of the carbon atoms at the edges. In correspondence of each removed atom, we have imposed a hopping parameter equal to zero.

A point charge approximation has been instead assumed for ionized impurities in the dielectric with a nominal concentration equal to n_{IMP}, and randomly distributed on a plane 0.2 nm far from the nanoribbon as in [10].

Phonon-limited mobility (both acoustic and optical) has been computed by means of a semi-analytical model as in [6], but extending the Kubo-Greenwood formalism beyond the effective mass approximation, considering the tight-binding energy dispersion relations and accounting for energy relaxation at GNR edges. Neglecting the contribution of inter-subband scattering, phonon-limited mobility of a 1D conductor can be expressed as a sum over all contributing subbands j [11]:

$$\mu = \frac{2q}{\pi\hbar\, n_{2D_{TOT}} W k_B T} \sum_j \int_{E_{Cj}}^{+\infty} dE\, \tau_{Pj}(E) \frac{f(E)\,[1-f(E)]}{E - E_{Cj} + E_{Cj0}} \cdot \left(\frac{E_{Cj0}}{m_j} \left[(E - E_{Cj} + E_{Cj0})^2 - E_{Cj0}^2 \right] \right)^{1/2}, \tag{2}$$

where $n_{2D_{TOT}}$ is the total electron density, τ_{Pj} is the momentum relaxation time on the j-th subband, W the GNR width, $f(E)$ the Fermi factor, E_{Cj} is the cut-off energy of the j-th subband, which reduces to E_{Cj0} for a zero gate voltage [12] and T is the temperature. According to [12], the effective

electron mass m_j on the j-th subband reads

$$m_j(E) = -\frac{2}{3}\frac{\hbar^2 E_{Cj0}}{a^2 t^2 A_m}\,, \tag{3}$$

where t is the hopping parameter (2.7 eV) and $A_m = cos(\pi m/(N+1))$, where N is the number of dimer lines of the GNR. For the first conduction subband $E_{Cj0} = E_g/2$, where E_g is the energy gap and m (which runs from 1 to N) is the index for which A_m is closer to -1/2 [12].

Scattering rates are evaluated as in Ref. [6], by means of the Fermi's golden rule [13] and expressing the GNR electronic wave functions as a combination of states in the K and K' valleys of the underlying 2D graphene band structure. The optical phonon scattering rate reads:

$$\frac{1}{\tau_{OPj}(E)} = \frac{n^{\pm}\pi D_{OP}^2}{4\rho W \omega_{LO}}\rho_{1Dj}(E \pm \hbar\omega_{LO})\,, \tag{4}$$

where $n^- = 1/[exp(\hbar\omega_{LO}/k_BT) - 1]$ and $n^+ = n^- + 1$ are the Bose-Einstein occupation factors for one-phonon annihilation and creation processes, respectively, $\hbar\omega_{LO}$ is the phonon energy, D_{OP} is the optical deformation and $\rho = 7.6 \times 10^{-8}$ g/cm^2 is the 2D density of graphene. The acoustic phonon scattering rate reads instead:

$$\frac{1}{\tau_{ACj}(E)} = \frac{n_{ph}\pi D_{AC}^2 q_z}{4\rho W \omega_{AC}}\rho_{1Dj}(E)\,, \tag{5}$$

where $n_{ph} = n^+ + n^-$ is the total occupation factor, $D_{AC} = 16$ eV is the deformation potential of acoustic phonons, $\omega_{AC} = v_s\, q_z$ is the acoustic phonon frequency, $v_S = 2 \times 10^4$ m/s is the sound velocity of 2D graphene and $|q_z| = 2|k_{zj}|$ is the module of the phonon wavevector under the backscattering condition in the longitudinal direction. For what concerns the 1D density of states in GNRs, the following expression has been adopted for the DOS in the j-th subband [12]:

$$\rho_{1Dj}(E) = \frac{2}{\pi\hbar}\sqrt{\frac{m_j\,(E + E_{Cj0} - E_{Cj})^2}{|E_{Cj0}(E - E_{Cj})\,(E + 2E_{Cj0} - E_{Cj})|}}\,. \tag{6}$$

III. Results and Discussions

The simulated devices are 10 nm-long GNR-FETs embedded in a 2 nm thick SiO_2 dielectric. Different GNR widths W have been considered, ranging from 1 to 10 nm. In Fig. 1, we show a TEM picture of a graphene flake, where single-atom defects amount to about 1.1%. Figs. 2 shows a simulated GNR sample with a fraction of edge defects H of 20% (left) and with a defect concentration n_d of 2.5% (right).

LER-limited mobility as a function of W for different H is plotted in Fig. 3a. As predicted by the analytical model in [6], for $W < 5$ nm and for large H (20%), μ is proportional to W^4, while for wider GNRs and for smaller H, such a law does not hold. Mobility is proportional to $1/H$ for large W, as expected, whereas the dependence on H is steeper for narrower devices, since quantum localization becomes relevant. While for narrow GNR μ increases with n_{2D} (Fig. 3b), for wider GNR and in the strong inversion regime μ shows the opposite trend due to mode-mixing, as already observed also in SNW-FETs [14].

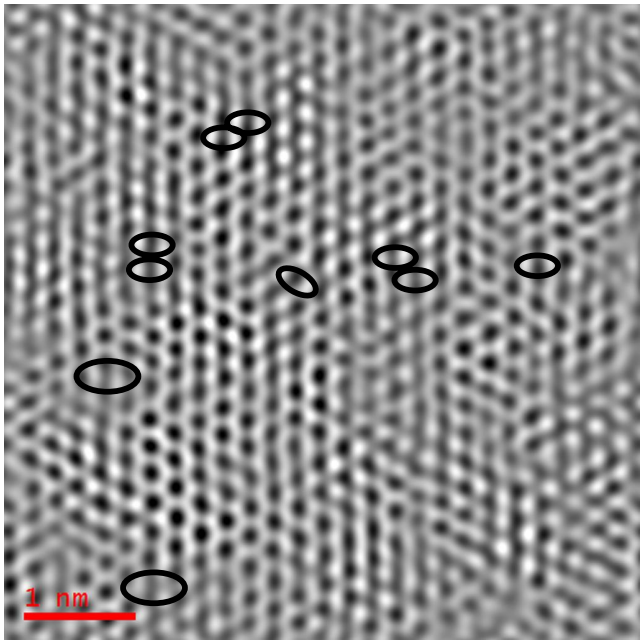

Fig. 1. TEM image of a graphene flake, where single vacancy defects are highlighted. The defect percentage of the sample is approximately 1.1%.

Defect-limited mobility is plotted in Fig. 4a as a function of W for different defect concentrations. Also in this case, localization suppresses mobility for narrower ribbons. As expected, for fixed defect density, mobility slightly increases with electron density. In Fig. 5 we show the inverse of mobility as a function of n_d. For $W = 10.10$ nm a linear dependence is observed with a slope close to that found in experiments for graphene [15], further validating our results.

Impurity-limited mobility is plotted in Fig 6a, as a function of W. According to [1], ionized impurities are one of the main limiting factors of GNR mobility. As previously performed in ab-initio calculations [10], we have considered a surface impurity distribution of positive charges equal to $+0.4q$ placed at 0.2 nm far from the GNR surface.

As can be noted, even a reasonably high impurity concentration of 10^{12} cm^{-2} yields large mobilities (10^4 cm^2/Vs). Smaller values of μ (1700 cm^2/Vs) are instead obtained for very narrow GNRs by increasing the impurity charge up to $+2q$, due to the strongly nonlinear impact on screening in the channel. Even in this case, localization strongly degrades mo-

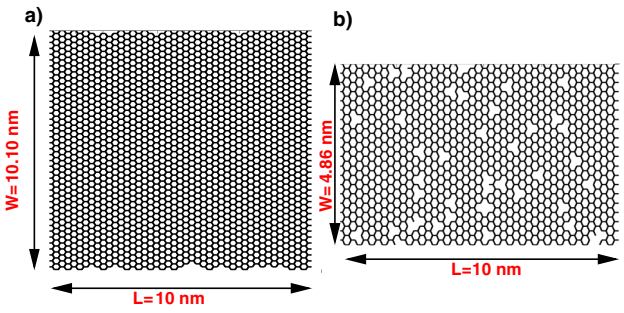

Fig. 2. Simulated 2D structure of a 10.10 nm wide GNR with a 20% concentration of edge roughness (a) and of a 4.86 nm wide GNR with a 2.5% defect concentration.

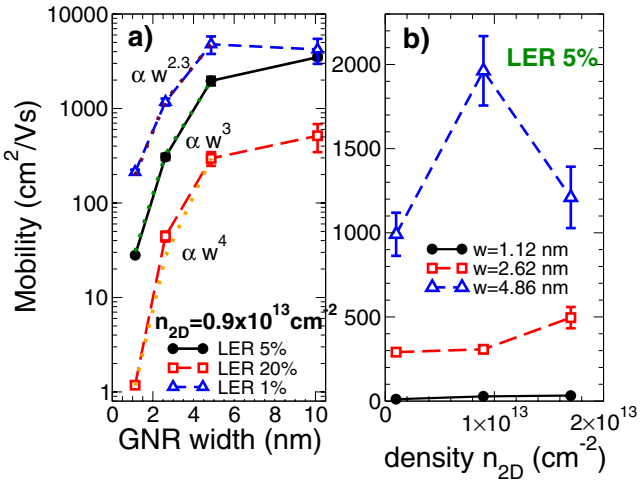

Fig. 3. a) LER-limited mobility as a function of W for $n_{2D} = 0.9 \times 10^{13}$ cm^{-2} and for different H. b) LER-limited mobility as a function of n_{2D} for $H = 5\%$.

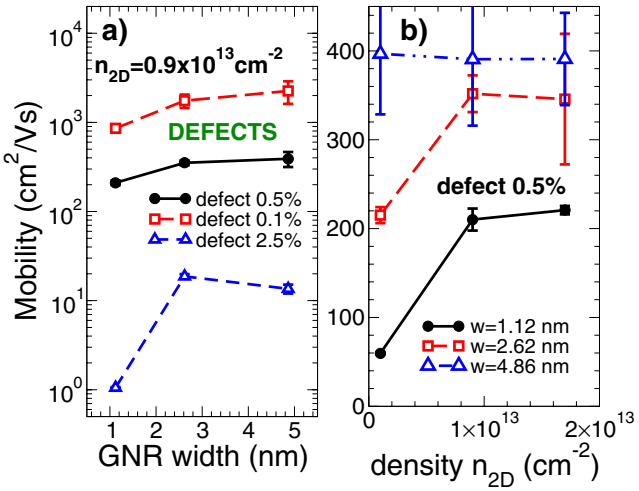

Fig. 4. a) Defect-limited mobility as a function of W for $n_{2D} = 0.9 \times 10^{13}$ cm^{-2} and for different defect fraction n_d. b) Mobility as a function of n_{2D} for a defect fraction $n_d = 0.5\%$.

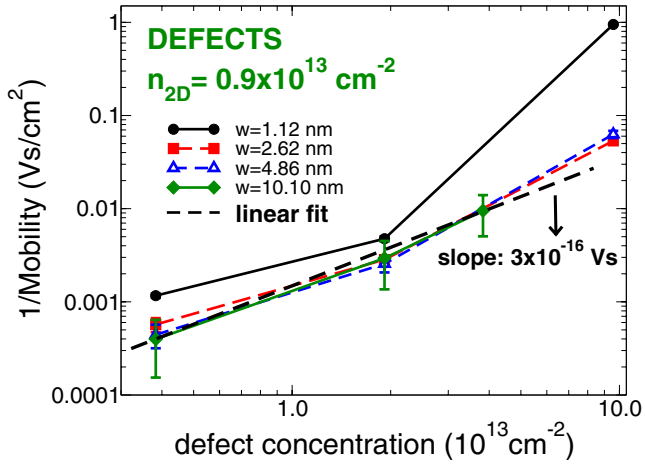

Fig. 5. Inverse mobility as a function of n_d for a fixed carrier density $n_{2D} = 0.9 \times 10^{13}$ cm^{-2} and for different GNR widths W.

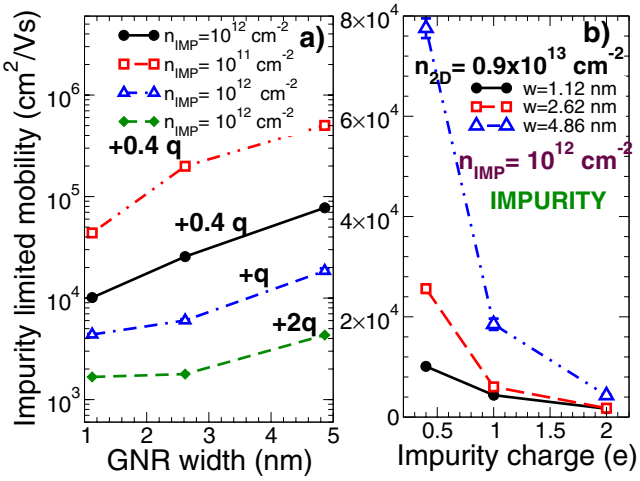

Fig. 6. a) Impurity-limited mobility as a function of W for different impurity concentration n_{IMP} and impurity charge. b) Mobility as a function of the impurity charge for $n_{IMP} = 10^{12}$ cm^{-2}. In both figures $n_{2D} = 0.9 \times 10^{13}$ cm^{-2}.

bility for narrower ribbons. Differently to [1], our numerical results seem to state that impurities are not the main limiting mechanism of mobility in GNR.

Phonon-limited mobility (optical and acoustic) are shown in Figs. 7 and 8, considering three subbands and two different sets of parameters, according to [6] ($\hbar\omega_{LO} = 160$ meV and $D_{OP} = 1.4 \times 10^9$ eV/cm) and to [7] ($\hbar\omega_{LO} = 62$ meV and $D_{OP} = 2.7 \times 10^9$ eV/cm), which corresponds to zone-boundary longitudinal optical phonons and ZO optical phonons, respectively. As can be noted in Fig. 8, the simple analytical approach is in really good agreement with results obtained by means of more sophisticated Monte Carlo simulations [7]. It is important to note that the obtained phonon-limited mobility is extremely sensitive to the considered parameters and that neglecting inter-subband scattering probably leads to an over estimation of mobility at large electron density.

Finally, we compare numerical results with the experiments shown in [5]. Good agreement are obtained using the scattering parameters in [7], and phonon scattering results to be the main limiting mechanism (Fig. 9). On the other hand, using the set in [6], one can reasonably reproduce the experiments only by considering LER with $H = 5\%$ and a defect concentration of 0.5% (Fig. 10).

IV. Final Remarks

In the extreme lack of experimental results on mobility in GNRs, atomistic simulations can help in understanding the functional dependences of mobility and the role of the different scattering mechanisms. Phonon-limited mobility has to be quantitatively understood on the basis of extensive characterization and modeling: in the narrower GNRs – most relevant from the point of view of device application – it can suppress mobility down to the value of mundane semiconductors.

V. Acknowledgments

Authors thank Dr. M. Lemme and Prof. P. Palestri for useful discussions, CINECA Super-Computing Center, Bologna, and www.nanohub.org for the provided computational resources. This work was supported in part by the EC 7FP through

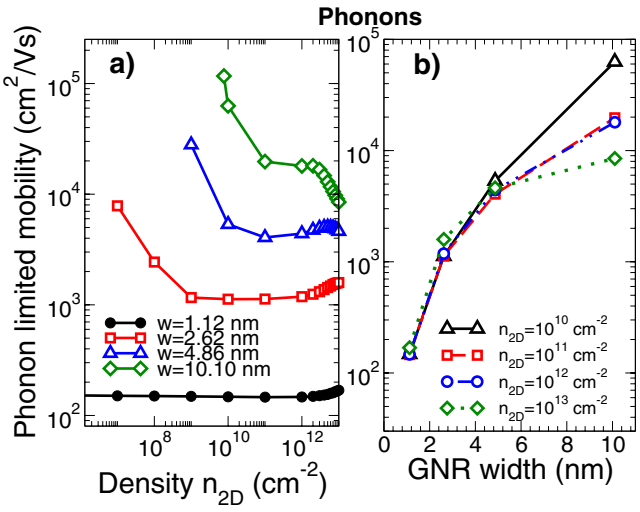

Fig. 7. a) Mobility limited by phonon scattering (optical+acoustic) as a function of n_{2D} for different W, computed with parameters from [6]. b) Mobility as a function of W for different electron density n_{2D}.

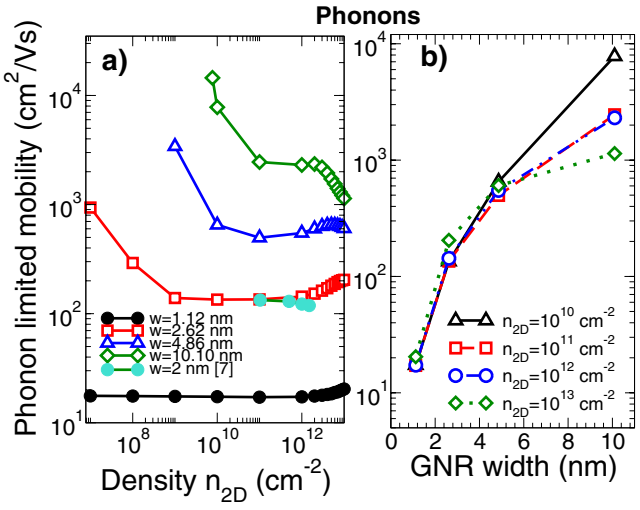

Fig. 8. a) Phonon-limited mobility (optical+acoustic) as a function of n_{2D} for different W computed with parameters from [7]. b) Mobility as a function of W in the subthreshold and in the above threshold regimes.

the Network of Excellence NANOSIL (Contract 216171), by the Project GRAND (Contract 215752) and by the European Science Foundation EUROCORES Programme Fundamentals of Nanoelectronics, through funding from the CNR (awarded to IEEIIT-PISA) and the EC 6FP, under Project Dewint (Contract ERASCT- 2003-980409).

REFERENCES

[1] J.-H. Chen et al., "Intrinsic and extrinsic performance limits of graphene devices on SiO_2", *Nature Nanotechnology*, Vol. 3, p. 206, 2008.
[2] X. Li et al., "Chemically Derived, Ultrasmooth Graphene Nanoribbon Semiconductors", *Science*, Vol. 319, p. 1229, 2008.
[3] Z. Chen and J. Appenzeller, "Mobility Extraction and Quantum Capacitance Impact in High Performance Graphene Field-effect Transistor Devices", *IEDM Tech. Digest*, p. 509, 2008.
[4] G. Fiori et al., "Simulation of Graphene Nanoribbon Field-Effect Transistors", *IEEE Electron Dev. Lett.*, Vol. 28, p. 760, 2007.
[5] X. Wang et al., "Room-Temperature All-Semiconducting Sub-10 nm Graphene Nanoribbon Field-Effect Transistors" *Phys. Rev. Lett.*, Vol. 100, p. 206803, 2008.
[6] T. Fang et al., "Mobility in semiconducting graphene nanoribbons: Phonon, impurity, and edge roughness scattering" *Phys. Rev. B*, Vol. 78, p. 205403, 2008.

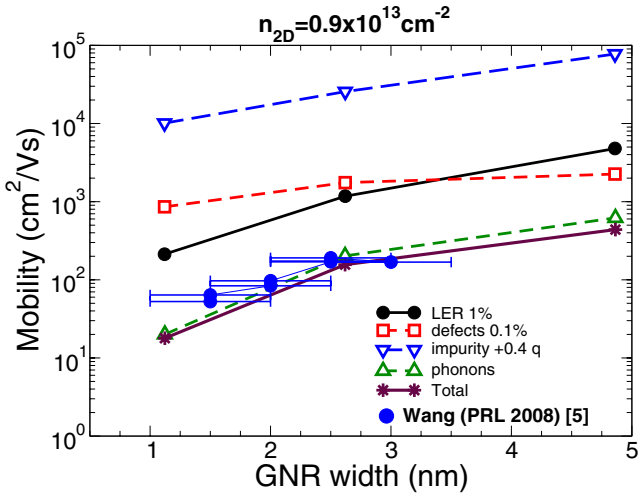

Fig. 9. Mobility limited by different scattering mechanisms as a function of W for an edge roughness concentration $H = 1\%$ and for a defect concentration equal to 0.1%. The parameters for the scattering rates have been taken equal to those in [7]. The total mobility is also reported.

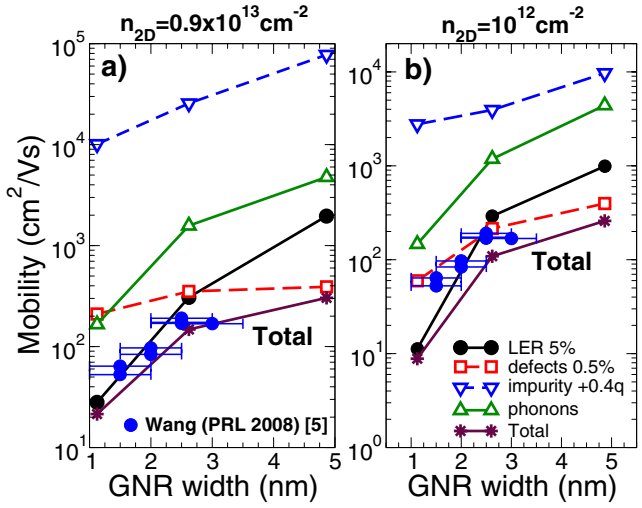

Fig. 10. Mobility limited by phonons, LER, defect and impurity scattering in the inversion regime for a LER concentration H=5%, $n_d = 0.5\%$, and two different electron densities. The parameters for the scattering rates have been taken from [6]. The experimental mobility from [5] is also reported in both figures, since corresponding electron concentration is not known.

[7] M. Bresciani et al., "A better understanding of the low-field mobility in Graphene Nano-ribbons", Proceedings ESSDERC'09, p. 480, 2009.
[8] Code and Documentation can be found at the URL: http://www.nanohub.org.tools/vides
[9] I. Deretzis et al., "A multiscale study of electronic structure and quantum transport in $C_{6n^n}H_{6n}$-based graphene quantum dots" http://arxiv.org/abs/0905.3122 (2009)
[10] K. Rytkönen et al., "Density functional study of alkali metal atoms and monolayers on graphite (0001)", *Phys. Rev. B*, Vol. 75, p. 075401, 2007.
[11] R. Kotlyar et al. "Assessment of room-temperature phonon-limited mobility in gated silicon nanowires", *Appl. Phys. Lett.*, Vol. 84, p.5270, 2004.
[12] P. Michetti and G. Iannaccone, "Analytical model of 1D Carbon-based Schottky-Barrier Transistors", http://arxiv.org/abs/0909.3736 (2009), *submitted to Trans. on Electron Devices*
[13] P. A. M. Dirac, "The Quantum Theory of Emission and Absorption of Radiation", *Proc. Roy. Soc. (London)*, Vol. A 114 (767), p. 243-265, 1927.
[14] S. Poli et al., "Size Dependence of Surface-Roughness-Limited Mobility in Silicon-Nanowire FETs", *IEEE Trans. Electron Devices*, Vol. 55, p. 2968-2976, 2008.
[15] J.-H. Chen et al., "Defect Scattering in Graphene", *Phys. Rev. Lett.*, Vol. 102, p. 236805, 2009.